

# Structural Analysis of Ribozymes

**Jonathan Ouellet**

*Department of Chemistry, Medical Technology and Physics, Monmouth University, West Long Branch, NJ, USA*

**Sirinart Ananvoranich**

*Department of Chemistry and Biochemistry, University of Windsor, Windsor, ON, Canada*

**Jean-Pierre Perreault**

*Department of Biochemistry, Université de Sherbrooke, Sherbrooke, QC, Canada*

	7.2	Cross-Linking	13
	7.3	Fluorescence	13
	7.4	In Vitro Evolution	13
<b>8</b>		<b>Three-Dimensional Structure</b>	<b>14</b>
	8.1	X-Ray Crystallography	14
	8.2	Nuclear Magnetic Resonance	14
	8.3	Molecular Modeling	14
<b>9</b>		<b>Conclusion</b>	<b>14</b>
		<b>Acknowledgments</b>	<b>15</b>
		<b>Abbreviations and Acronyms</b>	<b>15</b>
		<b>Related Articles</b>	<b>15</b>
		<b>References</b>	<b>15</b>

---

<b>1</b>	<b>Introduction</b>	<b>1</b>
<b>2</b>	<b>History</b>	<b>2</b>
<b>3</b>	<b>Synthesis of Ribonucleic Acid for Ribozyme Studies</b>	<b>2</b>
	3.1 In Vitro Transcription	2
	3.2 Chemical Synthesis	4
	3.3 Combination Method	6
<b>4</b>	<b>Primary Structure Information</b>	<b>6</b>
	4.1 Sequence Mapping and Self-Cleaving Activity	6
	4.2 Construction of Ribozymes and Their Variants	7
<b>5</b>	<b>Secondary Structure Determination</b>	<b>7</b>
	5.1 Computer-Aided Prediction	8
	5.2 Nuclease Mapping or Enzymatic Ribonucleic Acid Sequencing	8
	5.3 Chemical Interference	9
	5.4 Bioinformatics	10
<b>6</b>	<b>Analysis of Structure–Function Relationship</b>	<b>10</b>
	6.1 Cleavage Assay	10
	6.2 Metal Ion Dependence	11
	6.3 Kinetic Determination	11
	6.4 Nucleotide Analog Interference Mapping	12
<b>7</b>	<b>Global Three-Dimensional Structure and Folding</b>	<b>12</b>
	7.1 Binding Shift Assay	12

*Ribozymes are a family of ribonucleic acid (RNA) molecules that possess various catalytic capabilities. The various methodologies described in this article are presented in the order of their requirement for determination of the structure/function relationship of a ribozyme, beginning with the preparation of the RNA molecules required for the studies. Primary structure information is needed in order to identify potential ribozymes, whereas secondary and tertiary structures inform ribozyme characterization. The procedures described later are meant to guide investigators from the initial observation of RNA catalytic activity, i.e. ribozyme discovery, to the deduction of a structural model of the small RNA molecules. Here, hepatitis delta virus (HDV) ribozyme was used as a suitable model to illustrate the various steps involved in the structural analysis.*

## 1 INTRODUCTION

Ribozymes are a family of RNA molecules that possess various catalytic capabilities.<sup>(1–3)</sup> The best-known ribozymes are the endoribonucleases that are capable of cleaving RNA molecules at specific sequences. This group of ribozymes has tremendous potential for the development of a novel approach for the selective inactivation of specific RNA molecules, including both those derived from pathogenic viruses and those associated with inherited diseases.<sup>(4)</sup> The underlying theory of this inactivation is that the messenger ribonucleic acid (mRNA) encoding a harmful protein would be intercepted and destroyed by the ribozymes before that mRNA is translated.<sup>(5)</sup> In order to be able to fully exploit the potential of a ribozyme, it is crucial to have a complete understanding of the molecular mechanism of the ribozyme reaction. It has long been known that modification of RNA (ribozyme) structure often results in the alteration of its catalytic properties.

Update based on the original article by Sirinart Ananvoranich and Jean-Pierre Perreault, *Encyclopedia of Analytical Chemistry*, © 2000, John Wiley & Sons, Ltd

*Encyclopedia of Analytical Chemistry*, Online © 2006–2013 John Wiley & Sons, Ltd.

This article is © 2013 John Wiley & Sons, Ltd.

This article was published in the *Encyclopedia of Analytical Chemistry* in 2013 by John Wiley & Sons, Ltd.

DOI: 10.1002/9780470027318.a1427.pub2

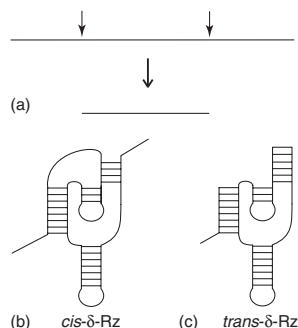


**Figure 1** The discovery and development of HDV ribozyme. (a) The single-stranded RNA genome of HDV is produced in a multimeric unit. Its self-cleaving motif is responsible for the release of multiple monomeric copies of the HDV genome, which are then re-circularized. (b) The HDV-cleaving motif was subsequently identified. (c) From secondary structure analysis, a trans-acting HDV ribozyme was derived by separating the junction between the P1 and P2 stems.

The various methodologies described in this article are presented in the order of their requirement for determination of the structure/function relationship of a ribozyme, beginning with the preparation of the RNA molecules required for the studies. Primary structure information is needed in order to identify potential ribozymes, whereas secondary and tertiary structures inform ribozyme characterization. The procedures described later are meant to guide investigators from the initial observation of RNA catalytic activity, i.e. ribozyme discovery, to the deduction of a structural model of the above-mentioned ribozyme.

We use HDV ribozymes as a model to illustrate the various steps involved in the structural analysis of ribozymes. HDV ribozymes were originally identified as a self-cleaving motif located on the single-stranded circular RNA genome of the HDV,<sup>(6)</sup> which replicates through a rolling circle mechanism involving only RNA intermediates. Replication is initiated by binding of the host RNA polymerase II to the parental RNA and results in the synthesis of a complementary multimeric copy of the HDV genome (Figure 1). The monomeric HDV genome is then released from this multimer, thanks to the catalytic activity of the RNA self-cleaving motif, henceforth, known as the HDV ribozyme. This intramolecular cleavage is an RNA autocatalytic reaction performed by a *cis*-acting ribozyme (Figure 1b). On the basis of subsequent secondary structure information, obtained by various investigators,<sup>(7–10)</sup> this motif has been modified into an intermolecular system (Figure 1c): the so-called *trans*-acting ribozyme system containing both a substrate and an enzyme molecule.

## 2 HISTORY

RNA catalysis was first identified in the RNA components of both the group I intron by Cech<sup>(11)</sup> and ribonuclease P (RNase P) by Altman<sup>(12)</sup> in the early 1980s. These seminal discoveries were the very first examples of enzymatic catalysis in the absence of any protein, and these catalytically active RNAs were dubbed ‘ribozymes’ (RNA enzymes). Over the past three decades, several ribozymes have been identified that possess various catalytic capabilities, enabling the modification of the phosphodiester bonds of their substrates. With the development of *in vitro* selection procedures, RNA molecules that catalyze a spectrum of reactions, for example, phosphorylation and ligation, have been identified.<sup>(1–3)</sup> Over the last decade, knowledge of the structure and mechanisms of known natural ribozymes has evolved more rapidly than the discovery of novel ribozymes. A notable exception is the discovery of the glmS ribozyme, a self-cleaving RNA located in the 5′-untranslated region of glmS mRNA of certain bacteria.<sup>(13)</sup> Emergence of affordable next-generation sequencing (i.e. also named deep-sequencing) has also expanded the number of genomic sequences, with the foreseeable discovery of additional natural ribozymes. Moreover, the rising fields of synthetic biology and riboswitches will also undoubtedly both contribute to the engineering of allosteric ribozymes.<sup>(14)</sup> Exciting ribozyme capabilities will thus continue to be uncovered over the decades to come.

## 3 SYNTHESIS OF RIBONUCLEIC ACID FOR RIBOZYME STUDIES

Ribozymes and their substrates can be produced by either *in vitro* transcription or chemical synthesis. The basic requirements and protocols for these two methods are described later.

### 3.1 *In Vitro* Transcription

This protocol makes use of enzymatic reactions catalyzed by purified bacteriophage T7 RNA polymerase, which uses DNA as a template.<sup>(15)</sup> The sequence immediately downstream of the T7 RNA promoter affects the transcript yield. Indeed, the +1 to +3 promoter sequence with nucleotides (nts) GGG or GGC affords the highest yield.<sup>(16)</sup> Large RNAs are routinely generated by this method. The model substrate of the HDV ribozyme, an 11-nt-long oligomer, is also produced by this method (Figure 2a). Owing to the propensity of T7 RNA polymerase to add one or more nontemplate nucleotides to the 3′-end of the resultant transcripts, the subsequent

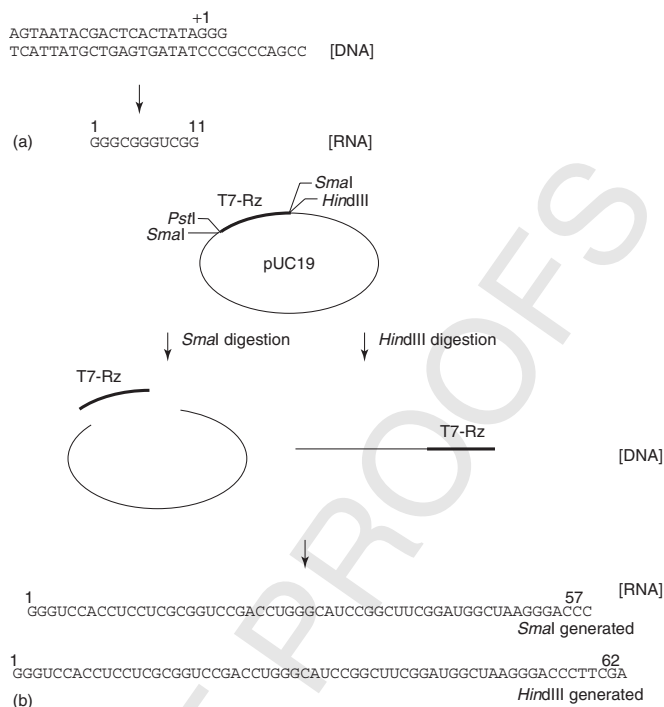


**Figure 2** DNA templates for in vitro transcription reactions catalyzed by bacteriophage T7 RNA polymerase. (a) The partial duplex formed by two oligonucleotides. The 11-nt substrate of the HDV ribozyme is illustrated. (b) The double-stranded DNA. The plasmid pUC19 harboring the sequence of trans-acting HDV ribozyme is digested with either *SmaI* or *HindIII*, and the resulting linear DNA is used as a template. RNA and DNA molecules are identified in square brackets.

purification and verification of both transcript length and sequence are required (Section 5.2). Design of self-cleaving ribozymes<sup>(17)</sup> or the use of methoxy moieties at the ribose C2' position at the penultimate nucleotide<sup>(18)</sup> significantly reduces the heterogeneity caused by the N+1 activity of T7 RNA polymerase. Affordability, ease, and rapidity of production of large quantities of RNA are the main advantages of this method. However, its main limitation is that specific modifications cannot be incorporated until the development of a transcription-efficient six-letter artificially expanded genetic information system (AEGIS).<sup>(19)</sup>

### 3.1.1 Oligonucleotide Templates

A pair of synthetic DNA oligonucleotide templates can be designed so that one contains the complementary sequences of both the T7 RNA promoter and the sequence coding for ribozyme or substrate, while the

other contains the forward sequence of the T7 RNA promoter (including the +1 to +3 GGG). Before the preparation of an in vitro transcription reaction mixture, the two oligonucleotides (500 pmol each) are mixed with Milli-Q ultrapure water (20  $\mu$ L) containing 10 mM tris(hydroxymethyl)aminomethane (Tris)-HCl, pH 7.5, 10 mM MgCl<sub>2</sub>, and 50 mM KCl, heated at 95 °C for 5 min, and allowed to cool slowly to 37 °C. The annealed partial duplexes formed then serve as templates for RNA synthesis by T7 RNA polymerase (Figure 2a).

### 3.1.2 Polymerase Chain Reaction Templates

Currently, synthetic DNAs tend to be of good quality and homogeneity as long as they do not exceed 80–90 nts in length. Thus, designing a DNA template from a partial duplex for a 150-nt-long RNA would be unwise. A rapid and efficient alternative is to create a double-stranded DNA template by elongating two DNA primers that can anneal onto each other's 3' end.

**3.1.2.1 Materials and Methods** Rapid, efficient, and cost-effective elongation polymerization of oligonucleotide primers can be performed via a few polymerase chain reaction (PCR) cycles, with DNA polymerase generating a full-duplex DNA product. In a final volume of 100  $\mu\text{L}$ , mix the following:

Forward DNA primer (100 $\mu\text{M}$ )	1 $\mu\text{L}$
Reverse DNA primer (100 $\mu\text{M}$ )	1 $\mu\text{L}$
dNTP (New England BioLabs Inc.) 2 mM each	10 $\mu\text{L}$
Taq DNA polymerase buffer (10 $\times$ ) (200 mM Tris-HCl, pH 8.8, 100 mM $(\text{NH}_4)_2\text{SO}_4$ , 100 mM KCl 1% Triton X-100)	10 $\mu\text{L}$
MgCl <sub>2</sub> (100 mM)	2 $\mu\text{L}$
Taq DNA polymerase (1 $\mu\text{g } \mu\text{L}^{-1}$ )	2 $\mu\text{L}$

As the elongation is very short, only five PCR cycles are required, wherein the reaction is successively incubated for 30 s at PCR temperatures of 94, 55, and 72  $^\circ\text{C}$ . Following the five cycles, extension is performed for 3 min at 72  $^\circ\text{C}$  to ensure the formation of complete double-stranded duplexes.

### 3.1.3 Cloned Templates

The HDV ribozyme DNA template was cloned into the pUC19 plasmid using recombinant DNA techniques (Section 4.2). The resultant recombinant plasmid containing the ribozyme sequence is then digested so as to either linearize or release the HDV ribozyme insert. T7 RNA polymerase uses the resultant DNA duplex as a template to produce transcripts extending until the end of the duplex or so-called 'run-off transcription' reactions<sup>(15)</sup> (Figure 2b).

**3.1.3.1 Materials and Methods** Mix the following in a final volume of 100  $\mu\text{L}$ .

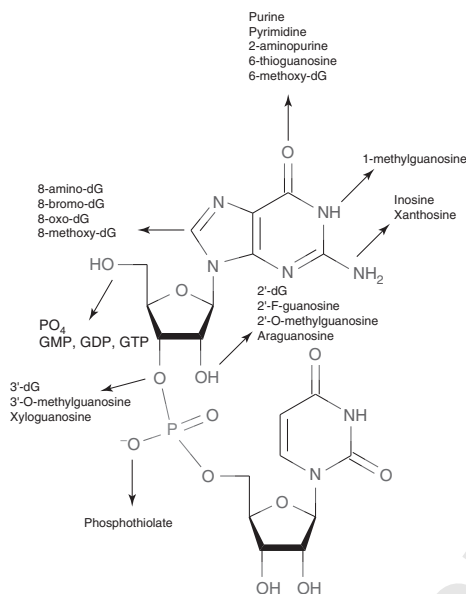
DNA template either as a partial duplex or PCR product (15 pmol) or as a digested cloned template (5 $\mu\text{g}$ )	20 $\mu\text{L}$
Murine ribonuclease inhibitor (New England BioLabs Inc.)	27 units
rNTP (New England BioLabs Inc.) 10 mM each	5 $\mu\text{L}$
Transcription buffer (5 $\times$ )	20 $\mu\text{L}$
400 mM <i>N</i> -(2-hydroxyethyl)piperazine- <i>N'</i> -ethanesulfonic acid (HEPES)-KOH, pH 7.5, 120 mM MgCl <sub>2</sub> , 10 mM spermidine, 100 mM dithiothreitol (DTT)	2 $\mu\text{L}$
Pyrophosphatase (1 unit $\mu\text{L}^{-1}$ , Sigma-Aldrich)	1 $\mu\text{L}$
Purified T7 RNA polymerase (2 $\mu\text{g } \mu\text{L}^{-1}$ )	2 $\mu\text{L}$

Incubate at 37  $^\circ\text{C}$  for 2–4 h. Add 5  $\mu\text{L}$  DNase I (RNase-free) (1 unit  $\mu\text{L}^{-1}$ , New England BioLabs Inc.) to eliminate the DNA template, then extract twice with buffered phenol:chloroform. Add 0.1 volume of 3 M sodium acetate, pH 5.2, and 2 volumes of ethanol to the aqueous phase. Chill for 15 min at  $-80^\circ\text{C}$  and centrifuge at 4  $^\circ\text{C}$  for 15 min in a microcentrifuge. Discard the supernatant, then add an equal volume of 70% ethanol, and repeat the centrifugation step. Dissolve the pellet in 20  $\mu\text{L}$  of Milli-Q ultrapure water and add 10  $\mu\text{L}$  of 5 $\times$  denaturing gel loading buffer (95% formamide, 10 mM ethylenediaminetetraacetic acid (EDTA), 0.05% bromophenol blue, and 0.05% xylene cyanol). Mixtures are fractionated by denaturing 20% polyacrylamide gel electrophoresis (PAGE, 19:1 ratio of acrylamide to bisacrylamide) containing 45 mM Tris-borate, pH 7.5, 7 M urea, and 1 mM EDTA. Reaction products are visualized by ultraviolet (UV) shadowing, bands corresponding to the correct sizes of the ribozymes and substrates are cut out, and the transcripts are eluted overnight at 4  $^\circ\text{C}$  in a solution (200  $\mu\text{L}$ ) containing 0.001% SDS, 0.1 mM EDTA, and 0.3 M sodium chloride. Transcripts are then precipitated by the addition of 0.1 volume of 3 M sodium acetate, pH 5.2, and 2.2 volumes of ethanol. Transcript yield is determined by spectrophotometry at 260 nm. Sequence and size of the RNA products are then verified by RNase digestion (Section 5.2).

## 3.2 Chemical Synthesis

RNA molecules can be chemically synthesized on solid supports in the same manner as DNA molecules, from 3' to 5', by taking advantage of the high chemical reactivity of the 5'-hydroxyl group. Enzymatic activity of the resultant RNA has been reported to be equivalent to that of RNA derived by transcription methods.<sup>(20)</sup> Most importantly, chemical synthesis allows the introduction of single-atom substitutions at specific positions in RNA molecules. There are three major targets for modification in chemogenetic studies of RNAs: the exocyclic base, the sugar, and the internucleotide phosphodiester linkage (Scheme 1).

The last decade has seen a new trend in RNA synthesis chemistry. 'Classical' RNA chemistry uses silyl-protective groups on the 2'-hydroxyl group of ribose bases,<sup>(21)</sup> and the 5'-hydroxyl group is protected by a DMT (4,4'-dimethoxytrityl) group. The work of Stephen A. Scaringe<sup>(22)</sup> helped provide better synthesis yields, purity, and ease of oligonucleotide deprotection by incorporating a silyl-protective group at the 5'-hydroxyl and an orthoester protective group at the 2'-hydroxyl.



**Scheme 1.** Specific modifications of an sRNA molecule.<sup>(23)</sup> Some modifications on the mononucleotide can be on the sugar or the base residue. The phosphodiester backbone can be modified to a phosphothiolate group.

RNA chemical synthesis strategies are based on the 2'-hydroxyl protective group. *t*-Butyldimethylsilyl (*t*BDMS) RNA synthesis chemistry protects the 2'-hydroxyl with a *t*BDMS group, whereas tri-*iso*-propylsilyloxymethyl (TOM) chemistry uses a TOM protective group; both being removable by treatment with fluoride ion. ACE chemistry uses a bis(acetoxyethoxy)methyl, while the silyl groups protect the ribose 5'-hydroxyl.

Efficiency of this new RNA chemical synthesis strategy has lowered the cost of synthetic RNA oligonucleotides. However, the cost of production is still prohibitive, especially when large RNA molecules or modifications are required. Owing to the high cost of equipment and materials, for most investigators, it is advisable to order custom-made RNA oligonucleotides from facilities such as Keck Oligonucleotide Synthesis Facility (Yale University, CT), Integrated DNA Technologies, Inc. (Coralville, IA), TriLink BioTechnologies (San Diego, CA), Bio-Synthesis Inc (Lewisville, TX), and the University of Calgary Oligo Service (Canada); a longer list is available on the Glen Research website.

### 3.2.1 *t*-Butyldimethylsilyl and Tri-*iso*-Propylsilyloxymethyl Chemistry

Most facilities offer synthesis scales with initial column capacities ranging from 100 nmol to 10  $\mu$ mol, while some solid-phase chemistry is capable of production in the 200  $\mu$ mol range. The choice of synthesis scale should take into consideration total RNA length. Each cycle of phosphoramidite addition includes a step of deblocking, coupling of the nucleoside phosphoramidite after its activation, capping, and oxidation. Standard coupling efficiency for each base is approximately 98–99.5%, resulting in cumulative effects and drastically reduced amounts of full-length product. For example, a 30-mer at 99% efficiency for each coupling would yield approximately three quarters of the initial column scale capacity, with only half of the synthesis product being full length with an efficiency of 98%. RNA synthesis over 60 nts in length with 2'-*O*-*t*-butyldimethylsilyl-5'-*O*-DMT-ribonucleosides (*t*BDMS-amidites) is not advisable. 2'-*O*-tri-*iso*-propylsilyloxymethyl-ribonucleosides (TOM-amidites) are used for RNA synthesis up to 90 nts in length.

In some cases, where longer RNA molecules are required, the investigator might combine T7 transcription and chemical synthesis (Section 3.3) in order to produce the desired RNA.

An automated DNA/RNA synthesizer (for example, ABI Model 394 from Applied Biosystem, Foster City, CA) is required for the synthesis of RNA oligonucleotides using *t*BDMS-amidites phosphoramidites, or TOM-amidites, in addition to nucleoside-functionalized controlled pore glass (CPG) or polystyrene supports (A, G, C, U). A wide variety of amidites allow various modifications to be incorporated into the synthesized RNA. For example, inosine can be introduced at selective positions. A 2'-deoxy or 2'-*O*-methyl RNA can be substituted for the 2'-OH of the ribose residue. The internucleotide phosphodiester bonds can be replaced by phosphothioate or phosphonate linkages. Moreover, other RNA modifications, such as biotin or fluorophore addition and halogenated deoxy and ribonucleotide incorporation, are aimed at facilitating the downstream use of the resulting RNAs.

Following their synthesis and cleavage from the solid support, RNA oligonucleotides are subjected to deprotection and desalting steps analogous to those performed for synthetic DNA oligonucleotides. The relatively harsh and extended deprotection step removes the 2'-*O*-protective silyl groups from the ribose residue by treatment with fluoride ion, using either tetrabutylammonium fluoride (TBAF) or triethylamine trihydrofluoride ( $\text{Et}_3\text{N}(\text{HF})_3$ ) according to the manufacturer's instructions;<sup>(24)</sup> the subsequent desalting step removes the inorganic salts,

trace organic compounds, low-molecular-weight impurities, and short failure sequences. The latter step can be performed using size-exclusion chromatographic columns such as G-25 Sephadex or reverse-phase high-performance liquid chromatography (HPLC) with an Ace 10 C18 column.<sup>(25)</sup> However, gel electrophoresis is the method of choice for removal of failure sequences. The sequence and size of the RNA products can be verified by RNase digestion (Section 5.2).

### 3.2.2 ACE Chemistry

Advances in amidite functional group protection made a considerable leap forward a decade ago. Rather than an amidite with an acid-labile protective group in 5' and a silyl-protective group in 2', which, respectively, require deprotection for every new coupling and at the end of synthesis, both protective groups were inverted. These new amidites allow RNA coupling yields similar to those of corresponding DNAs over a relatively short coupling time.

The industry (e.g. Thermo Fisher Scientific that acquired Dharmacon) provides the 2'-protected RNA oligonucleotide; a fast, simple, and mild deprotection releases the water-soluble protective group. Purification with PAGE or HPLC can then be performed.

2'-Acetoxyethoxy (2'-ACE) RNA synthesis chemistry allows the production of synthetic oligonucleotides of remarkable quality in large quantity. The main downside is the lack of amidites for chemogenetic studies. A majority of chemical modifications are available on amidites suitable for *t*BDMS chemistry.

### 3.3 Combination Method

RNAs produced by both enzymatic and chemical techniques can be combined in order to obtain long RNA molecules with site-specific modifications at affordable prices. For example, target RNA molecules with a specific phosphothiolate linkage isomer can be generated by enzymatic ligation of two individual RNAs, one of which is a chemically synthesized RNA containing a phosphothiolate linkage at the desired position. After separation of the resultant Sp and Rp isomers by HPLC, the desired RNA isomer is then traditionally joined to the other RNA by T4 RNA ligase.<sup>(26)</sup>

The joining of two RNA molecules is another area that has evolved over the last few years. Enzymatic ligation is still widely used, favored by new enzymes and better knowledge of substrate requirements. Enzymatic strategies include a DNA splint using T4 DNA ligase,<sup>(26)</sup> ssRNA ligation of two free RNA molecules,<sup>(27)</sup> in natural loops or induced loops using T4 RNA ligase,<sup>(28)</sup> and dsRNA nick-repair activity from T4 RNA Ligase II.<sup>(29)</sup>

An important downside of such enzymatic RNA ligation strategies for ribozyme studies is RNA ligase dependence to divalent metal ions, which induce cleavage of ligated RNA molecules. Chemical linkage of the two RNA strands alleviates the need for such divalent ions. For example, a disulfide bond can be created between a post-transcriptionally modified RNA and a synthetic RNA<sup>(30)</sup> or using click chemistry.<sup>(31)</sup>

## 4 PRIMARY STRUCTURE INFORMATION

Observation of self-cleaving RNA molecules naturally led to experiments aimed at identifying the causative element of cleavage, whether it lies with the sequence per se or its surroundings. In the case of HDV ribozymes, a linear dimer of the HDV genome was reported to be initially processed into a monomeric RNA when the responsible cDNA was transfected into a monkey kidney cell line.<sup>(6)</sup> These findings suggested that HDV RNA had either specific self-cleaving activity or an unusual secondary structure, allowing specific attack by a cellular RNase or specific self-cleaving activity. In order to locate the cleavage position, the self-cleaving motif of HDV was mapped on both strands of the HDV genome.<sup>(10)</sup> The steps required for this identification are described later.

### 4.1 Sequence Mapping and Self-Cleaving Activity

In general, cDNAs coding for RNA molecules of interest are generated and cloned into plasmids for identification using standard recombinant DNA techniques. Exonuclease III, a 3' to 5' exonuclease specific for double-stranded DNA carrying a blunt end, a 5'-overhang, or a nick, is commonly used for the construction of unidirectional nested deletion sets from plasmids. Nested deletion clones can be generated from either end using an appropriate restriction endonuclease that leaves either a blunt end or a 5'-overhang to linearize the DNA, followed by exonuclease III treatment. The sequence of each resulting deletion is determined by DNA sequencing.

RNA transcripts are then produced by *in vitro* transcription reactions in the presence of 20  $\mu$ Ci [ $\alpha$ -<sup>32</sup>P]UTP (PerkinElmer), purified, and subjected to various buffered conditions so as to identify the causative element of self-cleavage. To prove that self-cleaving activity is solely due to RNA transcripts and not to RNase or proteins present in the *in vitro* transcription reaction or cell extracts, the purified primary transcripts are incubated in 50 mM Tris-HCl, pH 8.0, and 10 mM MgCl<sub>2</sub>, i.e. standard conditions for many ribozyme cleavage assays, including HDV ribozymes.<sup>(10)</sup> The newly formed products are resolved on denaturing polyacrylamide gels

and visualized by gel exposure to either X-ray films or phosphorImaging™ screens.

To characterize the biochemical properties of the self-cleaving motif, cleavage efficiency is determined in various buffer systems (pH 5.0–9.0) containing either monovalent ( $\text{Na}^+$ ,  $\text{K}^+$ , or  $\text{NH}_4^+$ ) or divalent ions ( $\text{Mg}^{2+}$ ,  $\text{Ca}^{2+}$ , or  $\text{Mn}^{2+}$ ). The HDV ribozyme self-cleaving motif located on the HDV genome uses either  $\text{Mg}^{2+}$  or  $\text{Ca}^{2+}$  as a cofactor for efficient cleavage in Tris–HCl, pH 5.0–8.0,<sup>(10)</sup> or with other ions.<sup>(32)</sup> The cleavage products were identified as a 3' fragment with a 5'-hydroxyl end and a 5' fragment with a 2',3'-cyclic phosphate terminus similar to the products of the other small ribozyme cleavage reactions.

#### 4.2 Construction of Ribozymes and Their Variants

In order to explore the enzymatic properties of a ribozyme, cDNA clones coding for the ribozymes are constructed using recombinant DNA techniques. From the primary structural information (i.e. the sequence and the cleavage site), deoxyoligonucleotides can be designed and synthesized for cloning purposes. The HDV ribozymes used in our studies were initially constructed

using four overlapping oligonucleotides (Figure 3). Several restriction sites were included in order to facilitate the creation of variant ribozymes. For example, ribozyme mutants carrying a single mutation in the P1 stem can be produced by digestion of the plasmid carrying the ribozyme with the restriction endonucleases, *RsrII* and *SphI*. Subsequent ligation of this predigested plasmid to new oligonucleotides having the altered sequence flanked by *RsrII* and *SphI* sites led to the production of the ribozyme variant.<sup>(33)</sup>

Cloning and sequencing every variant is a precise but tedious methodology. Nowadays, quality, efficiency, and low cost of DNA synthesis mean that two complementary synthetic DNA oligonucleotide strands can be annealed together for sequences shorter than 100 nts (Section 3.1.1) to generate mutants at a much higher rate.

## 5 SECONDARY STRUCTURE DETERMINATION

Secondary structure information of RNA molecules is generally considered to be a simplification of what is in fact a three-dimensional complex. RNA secondary

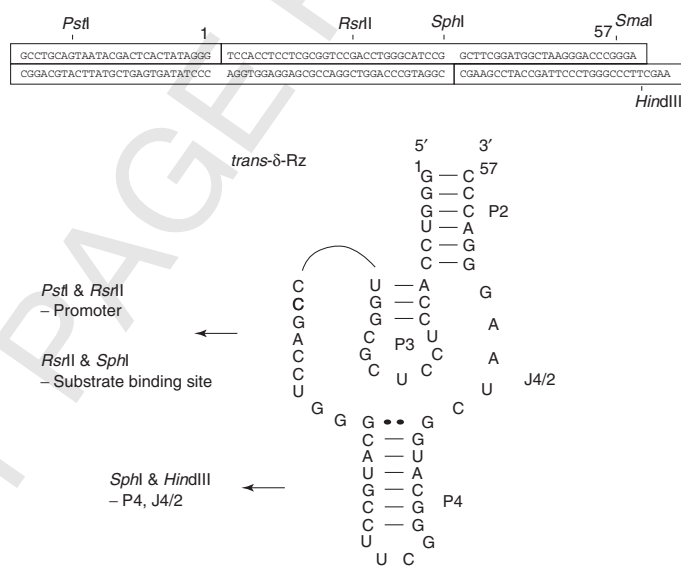


**Figure 3** Cloning of the trans-acting HDV ribozyme. Four overlapping oligonucleotides were designed so that they encode the entire sequence of trans-acting HDV ribozyme. Following the annealing of these four oligonucleotides, the resulting fragment was cloned into *PstI/HindIII*-digested pUC19. The resultant clone was verified by sequencing. The restriction endonuclease sites are identified on the double-stranded DNA.

structure is predicted using either computer-aided alignment or experimental data. Both approaches suggest putative base pairs that would eventually fold into a helix in the three-dimensional structure of the RNA molecule.

### 5.1 Computer-Aided Prediction

RNA secondary structure elucidation is similar to an alignment of protein, where the RNA sequence folds back onto itself rather than on complementary strands.<sup>(34)</sup> The complementary bases, G–C and A–U, form stable base pairs through hydrogen bonds between donor and acceptor sites on the bases, and are known as Watson–Crick base pairs. In addition, the weaker G–U wobble pair can be formed in a skewed manner. These three types of base pairs are called ‘canonical’ base pairs. Other base pairs (i.e. G–G or C–C) are called ‘noncanonical’ base pairs.<sup>(35)</sup> The prediction of secondary structure can be made from a single RNA sequence by minimizing the free energy of folding<sup>(36)</sup> obtained from a common folding pattern observed for a family of aligned, homologous RNAs. To calculate the free energy of RNA folding, arbitrary energy profiles are assigned to each individual base pair type and motif.<sup>(34)</sup> For the past two decades, the formulae defined by Turner and coinvestigators<sup>(34)</sup> have been widely used to define the free energy of stacking of canonical base pairs, hairpin loops, and both interior and bulge loops. In general, the secondary structure information obtained using aligned RNA sequences is very valuable because the RNA secondary structure is considered to be conserved to a greater degree than the primary sequence is. Over a period of sequence drift, the structural similarity might remain essentially the same through the phenomenon known as compensatory mutations, which conserve the base pairs,<sup>(34)</sup> as is observed in the structures of transfer RNAs (tRNAs) or ribosomal 5S RNA.

### 5.2 Nuclease Mapping or Enzymatic Ribonucleic Acid Sequencing

Enzymatic RNA sequencing is generally used in both the mapping of RNA secondary structures and in the determination of RNA length. This method takes advantage of the cleavage specificity of a variety of ribonucleases (RNases) and nucleases (Table 1) that are incubated with the substrate RNA in separate reactions.<sup>(37)</sup> The reaction mixtures are then fractionated by denaturing PAGE. The resulting bands are compared to an RNA ladder generated from the same RNA. To determine the length of the RNA, several nucleases can be used (Table 1).

#### 5.2.1 Materials and Methods

##### 5.2.1.1 5'-Dephosphorylation of Ribonucleic Acids

Mix the following in total volume of 20  $\mu\text{L}$ .

RNA purified from in vitro transcription reaction (10 pmol $\mu\text{L}^{-1}$ )	2 $\mu\text{L}$
Antarctic phosphatase (New England BioLabs Inc.)	5 units
10 $\times$ Antarctic phosphatase reaction buffer	2 $\mu\text{L}$
RNase-free water	

Incubate at 37  $^{\circ}\text{C}$  for 30 min. Perform heat inactivation for 5 min at 65  $^{\circ}\text{C}$ .

##### 5.2.1.2 5'-End-Labeling of Transcripts

Mix the following in total of 10  $\mu\text{L}$ .

Dephosphorylated RNA (1 pmol $\mu\text{L}^{-1}$ )	5 $\mu\text{L}$
10 $\times$ T4 polynucleotide kinase buffer (New England BioLabs Inc.)	1 $\mu\text{L}$
$\gamma$ - <sup>32</sup> P ATP (PerkinElmer, 10 $\mu\text{Ci} \mu\text{L}^{-1}$ )	3.2 pmol
T4 polynucleotide kinase (New England BioLabs Inc.)	10 units
RNase-free water	

Incubate at 37  $^{\circ}\text{C}$  for 30 min. Add 5  $\mu\text{L}$  of denaturing loading buffer (95% formamide, 10 mM EDTA, 0.05% bromophenol blue, and 0.05% xylene cyanol) and fractionate on a denaturing PAGE. The radioactively labeled RNA band is cut out following the exposure of the gel to an X-ray film or a phosphorimager screen printed at scale. The 5'-end-labeled RNA is eluted overnight at 4  $^{\circ}\text{C}$  in a solution (400  $\mu\text{L}$ ) containing 0.01% SDS and 0.5 M ammonium acetate and ethanol precipitated.

##### 5.2.1.3 Generation of a Ribonucleic Acid Ladder by Alkaline Hydrolysis

In a final volume of 5  $\mu\text{L}$ , mix the 5'-end-labeled RNA (5000–50 000 cpm  $\mu\text{L}^{-1}$ ) in a fresh solution containing 50 mM  $\text{NaHCO}_3$  and 5 mM EDTA. Incubate at 95  $^{\circ}\text{C}$  for 5 min. Add 5  $\mu\text{L}$  of denaturing loading buffer and 1  $\mu\text{L}$  of 0.5 M Tris–HCl, pH 7.5. Alternatively, 1  $\mu\text{L}$  of 0.1 M NaOH can be incubated with the RNA for 20 s at 90  $^{\circ}\text{C}$ .

##### 5.2.1.4 RNase T1 Digestion under Denaturing Conditions

In a final volume of 10  $\mu\text{L}$ , mix the 5'-end-labeled RNA (5000–50 000 cpm  $\mu\text{L}^{-1}$ ) with 1  $\mu\text{L}$  of 250 mM sodium citrate, pH 5.0, 2  $\mu\text{L}$  of denaturing loading buffer, and 1  $\mu\text{L}$  of RNase T1 (0.01 unit  $\mu\text{L}^{-1}$ ). Incubate at 55  $^{\circ}\text{C}$  for 10 min and stop the reaction by adding 6  $\mu\text{L}$  of chilled denaturing loading buffer.

**Table 1** Ribonucleases and nucleases that are commercially available, and are commonly used, are listed with their optimal buffers<sup>(38)</sup>

Nucleases	Cleavage	Buffers (5×)
Coefficient of variation (CV) or V1 Phy M S1	Prefers double-stranded RNA Ap↓N and Up↓N Single-stranded nucleic acid	125 mM Tris-HCl, pH 7.2 250 mM sodium citrate, pH 5.0 200 mM sodium acetate, pH 4.5, 1 M NaCl, 50 mM ZnSO <sub>4</sub>
T1 T2	Single-stranded RNA and Gp↓N Prefers single-stranded RNA and Ap↓N	250 mM sodium citrate, pH 5.0 250 mM sodium acetate, pH 5.0 250 mM Tris-HCl, pH 7.5
U2	Single-stranded RNA and Ap↓N	50 mM sodium citrate, pH 4.5

**5.2.1.5 Nuclease Assay** The specific cleavage by nucleases at the ribose-phosphate backbone is carried out using various buffering conditions, as listed in Table 1. Frequently, MgCl<sub>2</sub> or EDTA is also added in order to obtain conditions corresponding to either native or partially denatured folding. Note that the addition of heavy metal ions should be omitted in assays using RNase T2. Digestions are carried out for 1–10 min at room temperature or 37 °C, but the optimal time required for the mapping is dependent on the relative efficiency of each nuclease.<sup>(38)</sup> Cleavage reaction mixtures are fractionated by denaturing PAGE against corresponding RNA ladder and partial RNase T1 digestion.

### 5.3 Chemical Interference

Most chemical interference reactions rely on the accessibility of RNA functional groups. In its native 3D conformation, some RNA regions become flexible or accessible, while others are buried and, therefore, protected from chemical modification. Chemical reagents interact with heterocyclic bases, phosphodiester bonds, or ribose moieties, resulting in a modified RNA (Table 2).

Depending on the reaction, the effect of the RNA modification is monitored either directly or indirectly. When the modification results in RNA cleavage, the reaction can be monitored using 5'-end-labeled RNA fragments analyzed directly by fractionation by denaturing PAGE. Many chemical compounds modify RNA in such a way that enzymes, such as reverse transcriptase, are halted at the modified nucleotide. Modified residues are then detected by primer extension.

#### 5.3.1 Ribonucleic Acid Cleavage

Hydroxyl radicals interact nonspecifically with nucleic acids and correlate well with solvent accessibility at riboses. Generally, hydroxyl radicals are generated by the Fenton reaction using metals chelated in solution, such as Fe(II)-EDTA. Consequently, Fe(II)-EDTA

is often used for elucidation of the surface residues of an RNA molecule. These interactions occur at the heterocyclic bases and ribose residues, the latter of which result in strand breaks that are detected following gel fractionation. Just as for Fe(II)-EDTA, imidazole cleavage products do not require primer extension in order to resolve the reaction products. Imidazole and its conjugates rapidly cleave the phosphodiester bonds located in single-stranded regions, whereas those located in double-stranded regions are cleaved much more slowly.<sup>(38)</sup> For HDV ribozymes, several research groups have used RNase mapping, chemical interference, and UV cross-linking procedures to determine HDV ribozyme structures.<sup>(39–42)</sup>

In addition to secondary structure information, certain chemicals allow for probing high-affinity metal-ion-binding sites. For example, rather than generally producing hydroxyl radicals, as with Fe(II)-EDTA, they can be generated locally, close to a divalent ion-binding site.

The uranyl(VI) ion binds high-affinity metal-binding sites in RNA. Irradiation of the complex with visible light generates hydroxyl radicals, inducing cleavage in the vicinity of the metal-ion-binding site. Uranyl photocleavage has been used to map the metal-binding sites of the HDV ribozyme.<sup>(43)</sup> Another ion that competes with magnesium-binding sites is terbium. Tb<sup>3+</sup> binds with high affinity to similar sites on RNA, as does magnesium, resulting in the slow cleavage of the phosphodiester backbone, as shown for the HDV ribozyme.<sup>(44)</sup>

Another technique that is simple, yet highly informative of conformational changes in RNA structures, is in-line probing. Radioactive RNA is incubated for 48 h at room temperature with 20 mM MgCl<sub>2</sub> in buffered solution (pH 8.3). Single-stranded nucleotides are flexible and can transiently arrange the ribose's 2'-hydroxyl into an in-line attack conformation with the phosphate and the leaving group, resulting in backbone scission. The rigidity of RNA helices prevents such hydrolysis. This technique is

**Table 2** Chemical interference<sup>(38)</sup>

Chemicals	Attack at functional groups
Dimethyl sulfate	Adenosine (N1) and cytosine (N3)
CMCT	Uridine (N3) and guanosine (N1)
Kethoxal	Guanosine (N1 and N2) in single-stranded regions
DEPC	Purine (N7)
Fe(II)-EDTA	Heterocyclic bases and ribose
Imidazole and conjugates	Phosphodiester bonds
Benzoyl cyanide	2'-Hydroxyl
Ethyl nitrourea	Internucleotide phosphates and nucleophilic centers of heterocyclic bases

CMCT, 1-cyclohexyl-3-(2-morpholinoethyl)carbodiimide metro-*p*-toluene sulfonate; DEPC, diethylenepycarbonate.

extensively used to determine dissociation constants of ligands in riboswitches.<sup>(45)</sup>

### 5.3.2 Ribonucleic Acid Modification

DMS (dimethylsulfate), CMCT (1-cyclohexyl-3-(2-morpholinoethyl)carbodiimide metro-*p*-toluene sulfonate), and kethoxal are chemicals that modify certain exposed amino groups of specific nucleotides.<sup>(46)</sup> These modifications are then detected by real-time polymerase chain reaction (RT-PCR), revealing the secondary structure of the RNA.

Similarly to in-line probing, selective 2'-hydroxyl acylation reactions analyzed by primer extension (SHAPE)<sup>(47)</sup> also allows global determination of RNA structure. SHAPE reagent benzoylcyanide (BzCN) reacts with RNA hydroxyl functional groups to yield a stable ester when the nucleotide is accessible. The modified positions are determined by reverse transcription using a fluorescent primer or a radioactive primer as was the case for the HDV ribozyme SHAPE experiment.<sup>(48)</sup>

### 5.4 Bioinformatics

Sequenced genomes and transcriptomes provide tremendous amounts of structural information that still needs to be decrypted. When studying a new RNA sequence, base pair covariation and sequence conservation are key information for predicting secondary structure.

As the dominant structural elements in HDV ribozyme are helices, specific sequences are not conserved because the helices display sequence covariation. Thus, attempts at discovering new HDV-like ribozymes using alignment-based searches almost systematically failed. The discovery by SELEX of a HDV-like ribozyme within the second intron of the CPEB3 gene<sup>(49)</sup> raises the possibility of finding more instances of this ribozyme.

A search based on the secondary structure of the HDV ribozyme identified many new HDV-like ribozymes in a wide variety of organisms,<sup>(50)</sup> suggesting diverse biological roles for this self-cleaving RNA.<sup>(51)</sup>

## 6 ANALYSIS OF STRUCTURE-FUNCTION RELATIONSHIP

Using both intramolecular and intermolecular (i.e. with surrounding molecules) interactions, ribozymes adopt their native or tertiary structures and thereby gain catalytic activity. Surrounding molecules used in intermolecular interactions are metal ions, proteins, and water. During the first decade of HDV ribozyme discovery, there has been considerable progress in our understanding of the kinetics of RNA folding and cleavage because of simultaneous advances in both experimental and theoretical methods.<sup>(52)</sup> RNase mapping, chemical interference, and mutational analyses have been used to define the possible conformations of various RNA molecules. More recently, advanced techniques of crystallography, X-ray diffraction, and nuclear magnetic resonance (NMR) have determined precisely several RNA structures. Initially, the relationship between structure and function was most thoroughly studied for the group I intron-derived ribozyme.<sup>(53)</sup> Several of the approaches used in the study of this large ribozyme have also been applied to smaller ribozymes, the best studied of which are the hammerhead ribozymes. However, in some cases, structural information from different methods resulted in apparent discrepancies in the proposed structure-function relationship because of the conformational rearrangements needed for the catalysis to occur.<sup>(54)</sup> Kinetic characterization has been used widely in the survey of native structural analysis as it relates to enzymatic activity.

### 6.1 Cleavage Assay

A cleavage assay is the method of choice for demonstrating that a ribozyme has adopted its native structure. Cleavage assays can be carried out in buffered solution in the presence of trace amounts of radioactive labeled substrate. Radioactive RNA molecules are either the *cis*-ribozyme (RNA carrying a self-cleaving motif) or the substrate for a *trans*-ribozyme. The cleavage reactions catalyzed by both *cis*- and *trans*- $\delta$ -Rz require metal

ions as cofactors, i.e.  $\text{MgCl}_2$ ,  $\text{CaCl}_2$ , and  $\text{MnCl}_2$ . Denaturing agents such as formamide and urea are sometimes included in the reaction mixture in order to disturb any misfolded molecules and thereby enhance the refolding of the ribozyme–substrate complexes.

### 6.1.1 Materials and Methods

Mix, in total of 20  $\mu\text{L}$ , either radioactively labeled cis-acting ribozyme or radioactively labeled substrate of trans-acting ribozyme (ca. 50 000 cpm) in buffered solution containing 50 mM Tris–HCl, pH 7.5–8.0, and 5–50 mM  $\text{MgCl}_2$ . In the cases of trans-acting ribozyme, a fixed amount of ribozyme is added. The reaction is incubated for the time required (i.e. 10–30 min) and then stopped by adding 5  $\mu\text{L}$  of loading buffer (95% formamide, 0.05% bromophenol blue, and 0.05% xylene cyanol) for fractionation by denaturing PAGE (Figure 4a).

## 6.2 Metal Ion Dependence

In general, ribozymes require the presence of metal ions for folding and cleavage activity. Metal ions ( $\text{Mg}^{2+}$ ,  $\text{Ca}^{2+}$ ,  $\text{Mn}^{2+}$ ,  $\text{Sr}^{2+}$ , etc.) are added to cleavage reactions either in the presence or absence of monovalent ions ( $\text{Na}^+$ ,  $\text{K}^+$ , or  $\text{NH}_4^+$ ) in order to determine the metal ion requirement.<sup>(55)</sup>

## 6.3 Kinetic Determination

Time-course experiments are performed at various substrate and ribozyme concentrations in order to determine kinetic parameters such as maximum rate of cleavage and substrate association constant.

### 6.3.1 Single Turnover Conditions

Various amounts of ribozyme are mixed with trace amounts of substrate (final concentration < 1 nM) in an 18- $\mu\text{L}$  reaction mixture containing 50 mM Tris–HCl, pH 7.5, and are then subjected to denaturation by heating at 95 °C for 2 min. Mixtures are quickly placed on ice for 2 min and equilibrated to 37 °C for 5 min before the initiation of the reaction. Cleavage is initiated by the addition of  $\text{MgCl}_2$  to 10 mM final concentration. Reactions are incubated at 37 °C for 3.5 h or until the endpoint of cleavage is reached. Samples are quenched by the addition of 5  $\mu\text{L}$  stop solution (95% formamide, 10 mM EDTA, 0.05% bromophenol blue, and 0.05% xylene cyanol) and analyzed by 20% PAGE, as described earlier. Both the 11-nt substrate and the 4-nt reaction product bands are detected using a molecular dynamic radioanalytic scanner after exposure of the gels to a phosphorImaging™ screen (Figure 4a).

### 6.3.1.1 Measurement of Pseudo-First-Order Rate Constant ( $k_{\text{cat}}$ , $k_M$ , and $k_{\text{cat}}/k_M$ )

Kinetic analyses are performed under single-turnover conditions as described by Hertel et al.<sup>(56)</sup> with modifications in the ribozyme. Trace amounts of end-labeled substrate (<1 nM) are cleaved by various ribozyme concentrations (5–500 nM), and the fraction cleaved is determined. Rate of cleavage ( $k_{\text{obs}}$ ) is obtained from fitting of the data to the equation  $A_t = A_\infty(1 - e^{-kt})$ , where  $A_t$  is the percentage of cleavage at time  $t$ ,  $A_\infty$  is the maximum percent cleavage (or the endpoint of cleavage), and  $k$  is the rate constant ( $k_{\text{obs}}$ ). Each rate constant should be calculated from at least two measurements. Values of  $k_{\text{obs}}$  obtained are then plotted as a function of ribozyme concentration in order to determine the other kinetic parameters such as  $k_{\text{cat}}$ ,  $k_M$ , and  $k_{\text{cat}}/k_M$ .

### 6.3.2 Multiple Turnover Conditions

Trace amounts of labeled substrate are mixed with unlabeled substrate in order to obtain various substrate final concentrations. Fixed amounts of ribozyme (50 nM) are then added to the substrate mixtures in an 18- $\mu\text{L}$  reaction mixture containing 50 mM Tris–HCl, pH 7.5, and then subjected to denaturation by heating at 95 °C for 2 min. Again, the mixtures are quickly placed on ice for 2 min and equilibrated to 37 °C for 5 min before the initiation of the reaction. Cleavage is again initiated by the addition of  $\text{MgCl}_2$  to 10 mM.

### 6.3.3 Inhibition Analysis

The inhibitory effects of substrate and product can be kinetically tested under both single- and multiple-turnover conditions.

#### 6.3.3.1 Single-Turnover Conditions

Conditions similar to those described earlier can be used with various amounts of potential inhibitors (either substrate, product, or oligonucleotide). Reactions are initiated by mixing inhibitors (0.5–20  $\mu\text{M}$ ) with substrate (1 nM) before the addition of the ribozyme (50 nM) in 20  $\mu\text{L}$  of enzyme assay buffer (50 mM Tris–HCl, pH 8.0, 10 mM  $\text{MgCl}_2$ ). Aliquots (2  $\mu\text{L}$ ) are withdrawn at various intervals during the 40-min incubation period and are quenched by the addition of ice-cold stop solution (6  $\mu\text{L}$ ). Samples are fractionated by 10% denaturing PAGE, and reaction products are quantified following the exposure of gels to phosphorImaging™ screens. Control reactions are carried out in the absence of inhibitor. To evaluate the effect of an inhibitor on the intrinsic rate of ribozyme cleavage, data are analyzed as described by Clouet-d'Orval et al.<sup>(57)</sup> in order to determine the

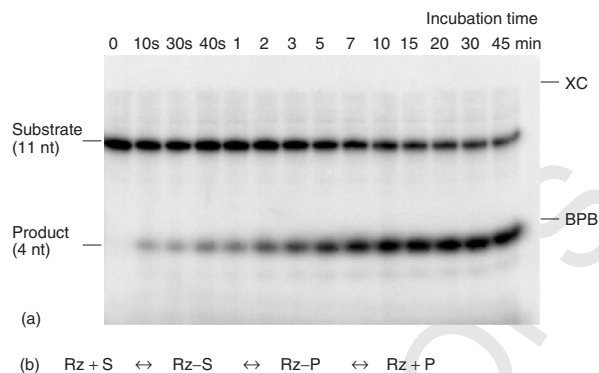


**Figure 4** Kinetic analysis of trans-acting HDV ribozyme. (a) An example of a time-course experiment. Trace amounts of 5'-end-labeled substrate were incubated with 100 nM ribozyme in a solution containing 50 mM Tris-HCl, pH 8.0, 10 mM MgCl<sub>2</sub>. (b) Simplified kinetic pathway of the cleavage reaction catalyzed by HDV ribozyme.

fraction of inhibition ( $I$ ) at each inhibitor concentration. Equation (1) is used and is represented as follows:

$$I = 1 - \left( \frac{k_2^{\text{inhibitor}}}{k_2} \right) \quad (1)$$

where  $k_2^{\text{inhibitor}}$  and  $k_2$  are the rates of cleavage in the presence and absence of the inhibitor, respectively. The values of  $k_2$  are obtained from fitting the experimental data to the pseudofirst-order rate equation (Equation 2):

$$A_t = A_\infty(1 - e^{-k_2 t}) \quad (2)$$

where  $A_t$  is the percentage of product formed at time  $t$  and  $A_\infty$  is the maximum amount of product formed. The fraction of inhibition ( $I$ ) is plotted versus inhibitor concentration, and the data fitted to a hyperbolic equation in order to obtain  $N_1$ , the inhibitor concentration needed to reduce the rate of cleavage by one half.

**6.3.3.2 Multiple-Turnover or Steady-State Conditions**  
Various concentrations of substrate are mixed with trace amounts of end-labeled substrate (<1 nM) so that final concentration ranges between 75 and 500 nM. Reaction mixtures contain substrate, ribozyme (50 nM), and inhibitor (0.5–20 μM), and are performed as described for single-turnover conditions. Cleavage rates ( $v_i$ , μM min<sup>-1</sup>) are determined at various substrate and inhibitor concentrations. Lineweaver–Burk, or reciprocal plots of  $1/v_i$  and  $1/[S]$  at all inhibitor ( $I$ ) concentrations, are plotted, and slopes and intercepts calculated by weighted linear regression analyses.

#### 6.4 Nucleotide Analog Interference Mapping

NAIM (Nucleotide Analog Interference Mapping) is a technique where a nucleotide analog is incorporated into the RNA sequence to evaluate the effects of its presence. In the case of the HDV ribozyme, the RNA was transcribed with various cytosine analogs that were incorporated randomly, followed by ribozyme cleavage activity assay.<sup>(58)</sup> Using cytosine analogs with different  $pK_a$  values shed light on the catalytic strategies of this ribozyme.

### 7 GLOBAL THREE-DIMENSIONAL STRUCTURE AND FOLDING

#### 7.1 Binding Shift Assay

Nondenaturing electrophoresis is commonly used in resolving the isomers that result from the folding of ribozymes. Moreover, kinetic parameters, such as equilibrium dissociation constant ( $K_d$ ), the association, and dissociation of substrate and product (Figure 5b), can be determined by this assay.<sup>(33)</sup>

##### 7.1.1 Materials and Methods

The equilibrium dissociation constants can be determined as follows. Various ribozyme concentrations, ranging from 5 to 600 nM, are individually mixed with trace amounts of end-labeled substrate (<1 nM) in a 9 μL solution containing 50 mM Tris-HCl, pH 7.5. This reaction is then heated at 95 °C for 2 min and cooled to 37 °C for 5 min before the addition of MgCl<sub>2</sub> to

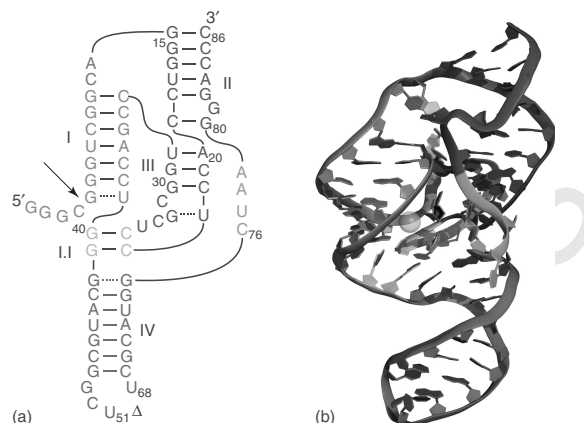


**Figure 5** HDV antigenomic (a) 2D and (b) 3D structures (MC-Sym). Secondary and tertiary structures of the antigenomic HDV ribozyme. The 3D model was built with MC-Sym using known biochemical features.<sup>(48)</sup> The arrow or the green sphere corresponds to the cleavage site.

a final concentration of 10 mM in a manner similar to that of a regular cleavage reaction. Reactions are incubated at 37 °C for 1.5 h, at which point 2  $\mu$ L of sample loading solution (50% glycerol, 0.025% of each bromophenol blue, and xylene cyanol) is added and the resulting mixture fractionated by nondenaturing PAGE (20% acrylamide with a 19:1 ratio of acrylamide to bisacrylamide in 45 mM Tris–borate, pH 7.5, and 10 mM MgCl<sub>2</sub> buffer system). Gels are pre-run at 20 W for 1 h before the sample loading, while actual electrophoresis is carried out at 15 W for 4.5 h at room temperature. Quantification of bound and free substrate molecules is performed following the exposure of gels to a phosphorImaging™ screen.

## 7.2 Cross-Linking

One of the direct ways to show proximity between two nucleotides in a tertiary structure is to create a short covalent bond between them. The uridine analog 4-thiouridine was incorporated in the HDV ribozyme to identify nucleotides close from each other in its native form.<sup>(59)</sup> Upon UV irradiation, the 4-thiouridine creates covalent bonds between closely stacked nucleotide bases, and the cross-linked complex can be isolated by fractionation on 7 M urea PAGE, followed by identification of the crosslink site by alkaline hydrolysis.

## 7.3 Fluorescence

Fluorescence is a powerful technique to monitor RNA structure. The fluorescent guanine analog 2-aminopurine

is highly sensitive to local stacking interactions with other bases. It was used in one of the first direct experiments demonstrating a structural difference between pre- and postcleavage structures of the HDV ribozyme.<sup>(60)</sup> An even more precise technique is fluorescence resonance energy transfer (FRET), where even a small distance change (from 2 to 8 Å) between a donor and acceptor fluorophore results in a large FRET efficiency difference. FRET directly measures substrate binding and dissociation as well as the conformational changes induced by cleavage.<sup>(61)</sup> Current FRET technology has evolved rapidly over the last decade to allow detection of single fluorophores, allowing single-molecule FRET measurements.<sup>(62)</sup> The next few years promise exciting new insights with respect to that perspective.

## 7.4 In Vitro Evolution

Rather than studying native sequence variability or creating mutations by rational design, in vitro selection can be used for the identification of important residues in the structure of HDV ribozymes.<sup>(63)</sup> A pool of trans-acting ribozymes with sequences that have been randomized are produced from synthetic DNA templates using T7 RNA polymerase. In each selection cycle, the inactive ribozyme–substrate complexes can be separated from active complexes using a biotinylated substrate against avidin. Using this procedure, the nucleotides essential for maintenance of the activity of trans-acting HDV ribozymes were identified.<sup>(63)</sup> Moreover, a ligation strategy of the cleaved cis HDV ribozyme was also shown

to increase the potential sequence capabilities of the HDV ribozyme by SELEX.<sup>(64)</sup>

## 8 THREE-DIMENSIONAL STRUCTURE

In biomolecules, adoption of native tertiary structure is usually a requisite for any activity. Solving secondary structure implies closing the gap between primary and tertiary structures. The native 3D structure of a molecule provides interesting avenues for a better understanding of its function and mechanism, for designing inhibitors and effectors as well as for a variety of other experiments.

### 8.1 X-Ray Crystallography

RNA crystallography has had a huge impact on RNA structural biology. Despite some *caveats*, it remains the best way to determine a high-resolution structure. Following the elucidation of the initial crystal structure of tRNAs, ribozyme crystal structures were fundamental in pushing the boundaries of the technique. The first published crystal structure of genomic HDV ribozyme in 1998<sup>(65)</sup> became central to our current views of its structural and functional elements. Crystal structure directly identified the stem P1.1, causing the ribozyme to adopt a nested double-pseudoknot fold. Moreover, proximity of the cleavage site of a cytosine also provided insight about the mechanism of catalysis.<sup>(66)</sup>

### 8.2 Nuclear Magnetic Resonance

Although the HDV ribozyme is considered on the large side for NMR studies, a shorter (and active) version of the ribozyme was designed to provide evidences of conformational changes from pre- to postcleavage.<sup>(67)</sup> Chemical shift change upon protonation of the N3-imino nitrogen from the catalytic cytosine was used to determine its  $pK_a$  and, therefore, provide information on the catalytic mechanism.<sup>(68)</sup>

### 8.3 Molecular Modeling

Before a high-resolution crystal structure of the HDV ribozyme was available, many research groups created a model based on the known secondary structure as well as from tertiary contact information. Now that many high-resolution structures are available, the goal has become to create models of reactional intermediates.

#### 8.3.1 Macromolecular Conformation Symbolic Programming

True molecular dynamic simulations are not yet possible because of the calculation time involved in all-atom RNA

folding. Programs use various strategies to simplify the problem and thus, reduce the number of calculations. Macromolecular conformation symbolic programming (MC-Sym)<sup>(69)</sup> uses cyclic building blocks extracted from crystallographic data to solve secondary structure constraints. Using homology features, a model of the antigenomic HDV ribozyme was built with MC-Sym (Figure 5), as well as some short-lived intermediates that would occur during the folding pathway.<sup>(48)</sup>

#### 8.3.2 Molecular Dynamics

Crystal structure provides a so-called snapshot among the many different possible conformations that occur over an entire catalytic cycle. Some crystals are obtained with nucleotide or metal analogs to mimic the transition state, but all states from the whole turnover cannot be represented at high resolution. However, there are molecular dynamic simulation software packages that calculate various conformational trajectories of RNAs using biochemical experiments as refinement. All the intermediates of the reaction can thus be modeled<sup>(70)</sup> or specific tasks, such as the positioning of the magnesium ion during the catalysis, can be performed.<sup>(71)</sup>

#### 8.3.3 Folding Pathway Simulation

A body of evidences<sup>(60,61,67,72)</sup> suggests global conformational changes from the pre- to postcleavage structures during HDV ribozyme catalysis. Once the various key steps have been identified and modeled by molecular dynamic simulation, it is possible to morph one structural state to the other, and to the next, until turnover is completed.<sup>(48)</sup> Because of the timescale issue, these simulations are a convenient visualization tool rather than an accurate representation of the actual conformational changes during catalysis. After all, RNA takes can take a million different paths to achieve catalysis.

## 9 CONCLUSION

In a little more than 20 years, both HDV ribozymes have been extensively mapped, resulting in a tremendous amount of structural data. Most structural characterizations have been confirmed by crystal structures providing even more structural insights and features. Some of the current apparent structural discrepancies may involve the dynamics of folding that create the essential intermediates needed to induce catalysis. Catalysis mechanistic may differ between the two ribozyme versions. The next few years will surely unlock the answers to these questions, not only for the HDV ribozyme, but for other ribozymes that provide the field of structural biology with invaluable tools.

**ACKNOWLEDGMENTS**

The authors thank the Canadian Institutes of Health Research (CIHR), previously the Medical Research Council of Canada (MRC), and the Natural Sciences and Engineering Research Council of Canada (NSERC) for providing operational and supporting grants, respectively. S.A. was a recipient of an NSERC postdoctoral fellowship. J.P.P. is a former MRC scholar; he formerly held the Canada Research Chair in Genomics and Catalytic RNA, and currently holds the Université de Sherbrooke Research Chair in Structure and Genomic RNA.

**ABBREVIATIONS AND ACRONYMS**

2'-ACE	2'-Acetoxyethoxy
<i>t</i> BDMS-amidites	2'- <i>O</i> - <i>t</i> -Butyldimethylsilyl-5'- <i>O</i> -DMT-ribonucleosides
<i>t</i> BDMS	<i>t</i> -Butyldimethylsilyl
AEGIS	Artificially Expanded Genetic Information System
BzCN	Benzoyl cyanide
CMCT	1-Cyclohexyl-3-(2-Morpholinoethyl)Carbodiimide Metro- <i>p</i> -Toluene Sulfonate
CPG	Controlled Pore Glass
DMS	Dimethylsulfate
DMT	4,4'-Dimethoxytrityl
DTT	Dithiothreitol
EDTA	Ethylenediaminetetraacetic Acid
FRET	Fluorescence Resonance Energy Transfer
HDV	Hepatitis Delta Virus
HEPES	<i>N</i> -(2-Hydroxyethyl)Piperazine- <i>N'</i> -Ethanésulfonic Acid
HPLC	High-Performance Liquid Chromatography
MC-Sym	Macromolecular Conformation Symbolic Programming
mRNA	Messenger Ribonucleic Acid
NAIM	Nucleotide Analog Interference Mapping
NMR	Nuclear Magnetic Resonance
nt	Nucleotide
PAGE	Polyacrylamide Gel Electrophoresis
PCR	Polymerase Chain Reaction
RNA	Ribonucleic Acid
RNase P	Ribonuclease P
RNase	Ribonuclease
RT-PCR	Real-Time Polymerase Chain Reaction

SHAPE	Selective 2'-Hydroxyl Acylation Reactions Analyzed by Primer Extension
TBAF	Tetrabutylammonium Fluoride
TOM-amidites	2'- <i>O</i> -Tri- <i>iso</i> -Propylsilyloxymethyl-Ribonucleosides
TOM	tri- <i>iso</i> -Propylsilyloxymethyl
Tris	Tris(hydroxymethyl)aminomethane
tRNA	Transfer RNA
UV	Ultraviolet

**RELATED ARTICLES***Nucleic Acids Structure and Mapping (Volume 6)*

Aptamers • Mass Spectrometry of Nucleic Acids • Nuclear Magnetic Resonance and Nucleic Acid Structures • Nucleic Acid Structural Energetics • RNA Tertiary Structure • Sequencing Strategies and Tactics in DNA and RNA Analysis • X-ray Structures of Nucleic Acids

a1402
a1416
a1417
a1418
a1428
a1429
a1419

**REFERENCES**

- J.C. Cochrane, S.A. Strobel, 'Catalytic Strategies of Self-cleaving Ribozymes', *Acc. Chem. Res.*, **41**, 1027 (2008).
- D.M. Lilley, 'Catalysis by the Nucleolytic Ribozymes', *Biochem. Soc. Trans.*, **39**, 641 (2011).
- A.R. Ferre-D'Amare, W.G. Scott, 'Small Self-cleaving Ribozymes', *Cold Spring Harb. Perspect. Biol.*, **2**, a003574 (2010).
- L. Scherer, J. Rossi, Cancer Therapeutic Applications of Ribozymes and RNAi in *Cancer Gene Therapy*, eds. D. Curiel, J. Douglas, Humana Press, Totowa, NJ, 51, 2005.
- S. Laine, R.J. Scarborough, D. Levesque, L. Didierlaurent, K.J. Soye, M. Mougel, J.P. Perreault, A. Gatignol, 'In Vitro and In Vivo Cleavage of HIV-1 RNA by New SOFA-HDV Ribozymes and Their Potential to Inhibit Viral Replication', *RNA Biol.*, **8**, 343 (2011).
- H.N. Wu, Y.J. Lin, F.P. Lin, S. Makino, M.F. Chang, M.M. Lai, 'Human Hepatitis Delta Virus RNA Subfragments Contain an Autocleavage Activity', *Proc. Natl. Acad. Sci. U. S. A.*, **86**, 1831 (1989).
- M.G. Belinsky, G. Dinter-Gottlieb, 'Non-Ribozyme Sequences Enhance Self-cleavage of Ribozymes Derived from Hepatitis Delta Virus', *Nucleic Acids Res.*, **19**, 559 (1991).
- A.D. Branch, H.D. Robertson, 'Efficient Trans Cleavage and a Common Structural Motif for the Ribozymes of the Human Hepatitis Delta Agent', *Proc. Natl. Acad. Sci. U. S. A.*, **88**, 10163 (1991).

9. A.T. Perrotta, M.D. Been, 'A Pseudoknot-like Structure Required for Efficient Self-cleavage of Hepatitis Delta Virus RNA', *Nature*, **350**, 434 (1991).
10. H.N. Wu, Y.J. Wang, C.F. Hung, H.J. Lee, M.M. Lai, 'Sequence and Structure of the Catalytic RNA of Hepatitis Delta Virus Genomic RNA', *J. Mol. Biol.*, **223**, 233 (1992).
11. B.L. Bass, T.R. Cech, 'Specific Interaction Between the Self-splicing RNA of Tetrahymena and its Guanosine Substrate: Implications for Biological Catalysis by RNA', *Nature*, **308**, 820 (1984).
12. C. Guerrier-Takada, S. Altman, 'Catalytic Activity of an RNA Molecule Prepared by Transcription In Vitro', *Science*, **223**, 285 (1984).
13. W.C. Winkler, A. Nahvi, A. Roth, J.A. Collins, R.R. Breaker, 'Control of Gene Expression by a Natural Metabolite-responsive Ribozyme', *Nature*, **428**, 281 (2004).
14. A. Saragliadis, B. Klausner, J.S. Hartig, 'In Vivo Screening of Ligand-dependent Hammerhead Ribozymes', *Methods Mol. Biol.*, **848**, 455 (2012).
15. J.F. Milligan, D.R. Groebe, G.W. Witherell, O.C. Uhlenbeck, 'Oligoribonucleotide Synthesis Using T7 RNA Polymerase and Synthetic DNA Templates', *Nucleic Acids Res.*, **15**, 8783 (1987).
16. D. Imburgio, M. Rong, K. Ma, W.T. McAllister, 'Studies of Promoter Recognition and Start Site Selection by T7 RNA Polymerase Using a Comprehensive Collection of Promoter Variants', *Biochemistry*, **39**, 10419 (2000).
17. J.M. Avis, G.L. Conn, S.C. Walker, 'Cis-acting Ribozymes for the Production of RNA In Vitro Transcripts with Defined 5' and 3' Ends', *Methods Mol. Biol.*, **941**, 83 (2012).
18. C. Kao, S. Rudisser, M. Zheng, 'A Simple and Efficient Method to Transcribe RNAs with Reduced 3' Heterogeneity', *Methods*, **23**, 201 (2001).
19. N. Morohashi, M. Kimoto, A. Sato, R. Kawai, I. Hirao, 'Site-specific Incorporation of Functional Components into RNA by an Unnatural Base Pair Transcription System', *Molecules*, **17**, 2855 (2012).
20. R. Vinayak, A. Andrus, A. Hampel, 'Rapid Desilylation of Oligoribonucleotides at Elevated Temperatures: Cleavage Activity in Ribozyme-substrate Assays', *Biomed. Pept. Prot. Nucl. Acids Struct. Synth. Biol. Act.*, **1**(227), (1995).
21. K.K. Ogilvie, N. Theriault, K.L. Sadana, 'Synthesis of Oligoribonucleotides', *J. Am. Chem. Soc.*, **99**, 7741 (1977).
22. S.A. Scaringe, F.E. Wincott, M.H. Caruthers, 'Novel RNA Synthesis Method Using 5'-O-Silyl-2'-O-Orthoester Protecting Groups', *J. Am. Chem. Soc.*, **120**, 11820 (1998).
23. W. Saenger, *Principles of Nucleic Acid Structure*, Springer-Verlag, New York, 1984.
24. M.J. Gait, *Oligonucleotide Synthesis a Practical Approach*, IRL Press, Oxfordshire; Washington, DC, Oxford, 1984.
25. I. Zlatev, M. Manoharan, J.J. Vasseur, F. Morvan, 'Solid-phase Chemical Synthesis of 5'-Triphosphate DNA, RNA, and Chemically Modified Oligonucleotides', in *Current Protocols in Nucleic Acid Chemistry*, ed. S.L. Beaucage Chapter 1, Unit 1, 28, 2012.
26. M.J. Moore, P.A. Sharp, 'Site-Specific Modification of pre-mRNA: the 2'-Hydroxyl Groups at the Splice Sites', *Science*, **256**, 992 (1992).
27. P.J. Romaniuk, O.C. Uhlenbeck, 'Joining of RNA Molecules with RNA Ligase', *Methods Enzymol.*, **100**, 52 (1983).
28. M.R. Stark, J.A. Pleiss, M. Deras, S.A. Scaringe, S.D. Rader, 'An RNA Ligase-mediated Method for the Efficient Creation of Large, Synthetic RNAs', *RNA*, **12**, 2014 (2006).
29. J. Nandakumar, S. Shuman, 'How an RNA Ligase Discriminates RNA Versus DNA Damage', *Mol. Cell*, **16**, 211 (2004).
30. D. Jaikaran, M.D. Smith, R. Mehdizadeh, J. Olive, R.A. Collins, 'An Important Role of G638 in the cis-Cleavage Reaction of the Neurospora VS Ribozyme Revealed by a Novel Nucleotide Analog Incorporation Method', *RNA*, **14**, 938 (2008).
31. A.H. El-Sagheer, T. Brown, 'New Strategy for the Synthesis of Chemically Modified RNA Constructs Exemplified by Hairpin and Hammerhead Ribozymes', *Proc. Natl. Acad. Sci. U. S. A.*, **107**, 15329 (2010).
32. K. Stokowa-Soltys, N. Gaggelli, J. Nagaj, W. Szczepanik, J. Ciesiolka, J. Wrzesinski, A. Gorska, E. Gaggelli, G. Valensin, M. Jezowska-Bojczuk, 'High Affinity of Copper(II) Towards Amoxicillin, Apramycin and Ristomycin. Effect of these Complexes on the Catalytic Activity of HDV Ribozyme', *J. Inorg. Biochem.*, **124**(26), (2013).
33. S. Ananvoranich, D.A. Lafontaine, J.P. Perreault, 'Mutational Analysis of the Antigenomic Trans-acting Delta Ribozyme: The Alterations of the Middle Nucleotides Located on the P1 Stem', *Nucleic Acids Res.*, **27**, 1473 (1999).
34. T. Xia, J.A. McDowell, D.H. Turner, 'Thermodynamics of Nonsymmetric Tandem Mismatches Adjacent to G.C Base Pairs in RNA', *Biochemistry*, **36**, 12486 (1997).
35. S. Halder, D. Bhattacharyya, *RNA structure and dynamics: a base pairing perspective*, Progress in Biophysics and Molecular Biology, 2013.
36. P. Agius, K.P. Bennett, M. Zuker, 'Comparing RNA Secondary Structures Using a Relaxed Base-pair Score', *RNA*, **16**, 865 (2010).
37. S. Quarrier, J.S. Martin, L. Davis-Neulander, A. Beauregard, A. Laederach, 'Evaluation of the Information Content of RNA Structure Mapping Data for Secondary Structure Prediction', *RNA*, **16**, 1108 (2010).

38. N.A. Kolchanov, I.I. Titov, I.E. Vlassova, V.V. Vlassov, 'Chemical and Computer Probing of RNA Structure', *Prog. Nucleic Acid Res. Mol. Biol.*, **53**, 131 (1996).
39. D.M. Chadalavada, A.L. Cerrone-Szakal, J.L. Wilcox, N.A. Siegfried, P.C. Bevilacqua, 'Mechanistic Analysis of the Hepatitis Delta Virus (HDV) Ribozyme: Methods for RNA Preparation, Structure Mapping, Solvent Isotope Effects, and Co-transcriptional Cleavage', *Methods Mol. Biol.*, **848**, 21 (2012).
40. P.K. Kumar, K. Taira, S. Nishikawa, 'Chemical Probing Studies of Variants of the Genomic Hepatitis Delta Virus Ribozyme by Primer Extension Analysis', *Biochemistry*, **33**, 583 (1994).
41. S.P. Rosenstein, M.D. Been, 'Evidence that Genomic and Antigenomic RNA Self-cleaving Elements from Hepatitis Delta Virus have Similar Secondary Structures', *Nucleic Acids Res.*, **19**, 5409 (1991).
42. L. Savochkina, V. Alekseenkova, T. Belyanko, M. Lukin, R. Beabealashvili, 'Properties of Antigenomic Hepatitis Delta Virus Ribozyme Cis- and Trans- Analogs', *Nucleosides Nucleotides Nucleic Acids*, **23**(935), (2004).
43. D. Wittberger, C. Berens, C. Hammann, E. Westhof, R. Schroeder, 'Evaluation of Uranyl Photocleavage as a Probe to Monitor Ion Binding and Flexibility in RNAs', *J. Mol. Biol.*, **300**, 339 (2000).
44. D.A. Harris, R.A. Tinsley, N.G. Walter, 'Terbium-mediated Footprinting Probes a Catalytic Conformational Switch in the Antigenomic Hepatitis Delta Virus Ribozyme', *J. Mol. Biol.*, **341**, 389 (2004).
45. E.E. Regulski, R.R. Breaker, 'In-line Probing Analysis of Riboswitches', *Methods Mol. Biol.*, **419**, 53 (2008).
46. S. Nishikawa, P.K. Kumar, Y.H. Jeoung, J. Kawakami, F. Nishikawa, Y. Suh, E. Ohtsuka, K. Taira, 'Chemical Probing Studies of the Hepatitis Delta Virus (HDV) Genomic Ribozyme', *Nucleic Acids Symp. Ser.*, 119 (1993).
47. S.A. Mortimer, K.M. Weeks, 'Time-Resolved RNA SHAPE Chemistry', *J. Am. Chem. Soc.*, **130**, 16178 (2008).
48. C. Reymond, D. Levesque, M. Bisailon, J.P. Perreault, 'Developing Three-dimensional Models of Putative-folding Intermediates of the HDV Ribozyme', *Structure*, **18**, 1608 (2010).
49. K. Salehi-Ashtiani, A. Lupták, A. Litovchick, J.W. Szostak, 'A Genomewide Search for Ribozymes Reveals an HDV-like Sequence in the Human CPEB3 Gene', *Science*, **313**, 1788 (2006).
50. C.H. Webb, N.J. Riccitelli, D.J. Ruminski, A. Lupták, 'Widespread Occurrence of Self-cleaving Ribozymes', *Science*, **326**, 953 (2009).
51. C.H. Webb, A. Lupták, 'HDV-like Self-cleaving Ribozymes', *RNA Biol.*, **8**, 719 (2011).
52. P.C. Turner, *Ribozyme Protocols*, Humana Press, Totowa, NJ, 1997.
53. B.L. Golden, A.R. Gooding, E.R. Podell, T.R. Cech, 'A preorganized Active Site in the Crystal Structure of the Tetrahymena Ribozyme', *Science*, **282**, 259 (1998).
54. K.F. Blount, O.C. Uhlenbeck, 'The Structure-Function Dilemma of the Hammerhead Ribozyme', *Annu. Rev. Biophys. Biomol. Struct.*, **34**, 415 (2005).
55. J. Wrzesinski, M. Legiewicz, B. Smolska, J. Ciesiolka, 'Catalytic Cleavage of Cis- and Trans-acting Antigenomic Delta Ribozymes in the Presence of Various Divalent Metal Ions', *Nucleic Acids Res.*, **29**, 4482 (2001).
56. K.J. Hertel, D. Herschlag, O.C. Uhlenbeck, 'A Kinetic and Thermodynamic Framework for the Hammerhead Ribozyme Reaction', *Biochemistry*, **33**, 3374 (1994).
57. B. Clouet-d'Orval, T.K. Stage, O.C. Uhlenbeck, 'Neomycin Inhibition of the Hammerhead Ribozyme Involves Ionic Interactions', *Biochemistry*, **34**, 11186 (1995).
58. A.K. Oyelere, J.R. Kardon, S.A. Strobel, 'pK(a) Perturbation in Genomic Hepatitis Delta Virus Ribozyme Catalysis Evidenced by Nucleotide Analogue Interference Mapping', *Biochemistry*, **41**, 3667 (2002).
59. J. Ouellet, J.P. Perreault, 'Cross-linking Experiments Reveal the Presence of Novel Structural Features Between a Hepatitis Delta Virus Ribozyme and its Substrate', *RNA*, **10**, 1059 (2004).
60. D.A. Harris, D. Rueda, N.G. Walter, 'Local Conformational Changes in the Catalytic Core of the Trans-acting Hepatitis Delta Virus Ribozyme Accompany Catalysis', *Biochemistry*, **41**, 12051 (2002).
61. M.J. Pereira, D.A. Harris, D. Rueda, N.G. Walter, 'Reaction Pathway of the Trans-acting Hepatitis Delta Virus Ribozyme a Conformational Change Accompanies Catalysis', *Biochemistry*, **41**, 730 (2002).
62. T. Ha, T. Enderle, D.F. Ogletree, D.S. Chemla, P.R. Selvin, S. Weiss, 'Probing the Interaction Between Two Single Molecules: Fluorescence Resonance Energy Transfer Between a Single Donor and a Single Acceptor', *Proc. Natl. Acad. Sci. U. S. A.*, **93**, 6264 (1996).
63. F. Nishikawa, H. Fauzi, S. Nishikawa, 'Detailed Analysis of Base Preferences at the Cleavage Site of a Trans-acting HDV Ribozyme a Mutation that Changes Cleavage Site Specificity', *Nucleic Acids Res.*, **25**, 1605 (1997).
64. A. Nehdi, J.P. Perreault, 'Unbiased In Vitro Selection Reveals the Unique Character of the Self-Cleaving Antigenomic HDV RNA Sequence', *Nucleic Acids Res.*, **34**, 584 (2006).
65. A.R. Ferré-D'Amaré, K. Zhou, J.A. Doudna, 'Crystal Structure of a Hepatitis Delta Virus Ribozyme', *Nature*, **395**, 567 (1998).
66. J.H. Chen, R. Yajima, D.M. Chadalavada, E. Chase, P.C. Bevilacqua, B.L. Golden, 'A 1.9 Å Crystal Structure of the HDV Ribozyme Precleavage Suggests both Lewis

- Acid and General Acid Mechanisms Contribute to Phosphodiester Cleavage', *Biochemistry*, **49**, 6508 (2010).
67. Y. Tanaka, M. Tagaya, T. Hori, T. Sakamoto, Y. Kurihara, M. Katahira, S. Uesugi, 'Cleavage Reaction of HDV Ribozymes in the Presence of  $Mg^{2+}$  is Accompanied by a Conformational Change', *Genes Cells: Devoted Mol Cell Mech*, **7**, 567 (2002).
68. A. Lupták, A.R. Ferre-D'Amare, K. Zhou, K.W. Zilm, J.A. Doudna, 'Direct pK(a) Measurement of the Active-site Cytosine in a Genomic Hepatitis Delta Virus Ribozyme', *J. Am. Chem. Soc.*, **123**, 8447 (2001).
69. M. Parisien, F. Major, 'The MC-Fold and MC-Sym Pipeline Infers RNA Structure From Sequence Data', *Nature*, **452**, 51 (2008).
70. T.S. Lee, G. Giambasu, M.E. Harris, D.M. York, 'Characterization of the Structure and Dynamics of the HDV Ribozyme at Different Stages Along the Reaction Path', *J. Phys. Chem. Lett.*, **2**, 2538 (2011).
71. N. Veeraraghavan, A. Ganguly, B.L. Golden, P.C. Bevilacqua, S. Hammes-Schiffer, 'Mechanistic Strategies in the HDV Ribozyme: Chelated and Diffuse Metal Ion Interactions and Active Site Protonation', *J. Phys. Chem. B*, **115**, 8346 (2011).
72. S. Ananvoranich, J.P. Perreault, 'The Kinetics and Magnesium Requirements for the Folding of Antigenomic Delta Ribozymes', *Biochem. Biophys. Res. Commun.*, **270**, 600 (2000).